applied sciences

MDPI

Article

Segmenting 20 Types of Pollen Grains for the Cretan Pollen Dataset v1 (CPD-1)

Nikos Tsiknakis [1,*], Elisavet Savvidaki [2], Sotiris Kafetzopoulos [3], Georgios Manikis [1], Nikolas Vidakis [3], Kostas Marias [1,3] and Eleftherios Alissandrakis [2]

1 Computational BioMedicine Laboratory, Institute of Computer Science, Foundation for Research and Technology Hellas—FORTH, 70013 Heraklion, Greece; gmanikis@ics.forth.gr (G.M.); kmarias@ics.forth.gr (K.M.)
2 Department of Agriculture, Hellenic Mediterranean University, 71004 Heraklion, Greece; elisavvidaki@hmu.gr (E.S.); ealiss@hmu.gr (E.A.)
3 Department of Electrical and Computer Engineering, Hellenic Mediterranean University, 71004 Heraklion, Greece; skafetzopoulos@gmail.com (S.K.); nv@hmu.gr (N.V.)
* Correspondence: tsiknakisn@ics.forth.gr

Abstract: Pollen analysis and the classification of several pollen species is an important task in melissopalynology. The development of machine learning or deep learning based classification models depends on available datasets of pollen grains from various plant species from around the globe. In this paper, Cretan Pollen Dataset v1 (CPD-1) is presented, which is a novel dataset of grains from 20 pollen species from plants gathered in Crete, Greece. The pollen grains were prepared and stained with fuchsin, in order to be captured by a camera attached to a microscope under a ×400 magnification. In addition, a pollen grain segmentation method is presented, which segments and crops each unique pollen grain and achieved an overall detection accuracy of 92%. The final dataset comprises 4034 segmented pollen grains of 20 different pollen species, as well as the raw data and ground truth, as annotated by an expert. The developed dataset is publicly accessible, which we hope will accelerate research in melissopalynology.

Keywords: dataset; honey; melissopalinology; pollen grain; segmentation

Citation: Tsiknakis, N.; Savvidaki, E.; Kafetzopoulos, S.; Manikis, G.; Vidakis, N.; Marias, K.; Alissandrakis, E. Segmenting 20 Types of Pollen Grains for the Cretan Pollen Dataset v1 (CPD-1). *Appl. Sci.* **2021**, *11*, 6657. https://doi.org/10.3390/app11146657

Academic Editor: Minjuan Wang

Received: 18 June 2021
Accepted: 19 July 2021
Published: 20 July 2021

1. Introduction

Honey is a natural food with great importance for many countries due to its nutritional and medicinal properties [1]. It is highly appreciated by consumers and the demand for honey of certified origin is currently a necessity. Pollen analysis, also known as melissopalynology, is a method to determine the origin of honey, based on the determination of the pollen grains presented in it [2]. Honey contains pollen as a result of the manipulation of the flower when honeybees collect nectar. The procedure largely followed today is based on the method described in [3]. Although widely accepted, this method has significant disadvantages, namely the high manual effort and the specialized expertise required, both leading to high costs and high demands on time and, thus, to restrictions in sample throughput [4]. Because of the high financial importance of honey, it is necessary to provide effective tools that can help ensure its origin.

The automation of this process could work directly, reducing the analysis time, whilst increasing the accuracy of the results. Procedures related to image analysis and the use of neural networks have yielded significant results. Recent years have seen advances in the fields of machine learning and artificial intelligence related to pollen analysis [5], with quite impressive results with up to 98% correct pollen classification [6].

Geographical indications (GIs) identify a good honey as one that originates from a particular place, has a particular quality, characteristic, or reputation [7]. In most cases, these indications have a determinative role in both domestic and international markets [8].

One such product is "Pefkothymaromelo Kritis PDO", a honey specific to Crete, which is characterized by specific organoleptic, physicochemical, and microscopic characteristics. To certify this product, pollen analysis is crucial. The main and defining type of pollen in that particular honey is thyme (formerly called *Coridothymus capitatus*, currently referred to as *Thymbra capitata*) which is present in all honey samples in a percentage greater than or equal to 10%. In addition, another 15 to 20 types of pollen grains from different plants are indicative of Cretan nature, mainly chestnut (*Castanea sativa*), heather (*Erica arborea*, *Erica manipuliflora*), eucalyptus (*Eucalyptus camaldulensis*), myrtle (*Myrtus communis*), different species of *Sinapis* sp. (Brassicaceae), carob (*Ceratonia siliqua*), giant fennel (*Ferula communis*) sage (*Salvia officinalis*), marjoram (*Origanum microphyllum*), and savory (*Satureja thymbra*) [9]. Therefore, an automated process of microscopic identification could aid the fast and accurate quality control of this product.

For this reason, a collection of pollen grains from plants usually present in "Pefkothymaromelo Kritis, PDO" was developed to create a microscopic imaging dataset. In particular, the scope of this work was to gather, prepare, and capture such images, as well as to develop an image processing method to segment each unique pollen grain. Doing so, the analysis of each pollen grain becomes easier, also enabling machine learning classification methods to be developed. The dataset is also publicly available at 10.5281/zenodo.4756360 (accessed on 13 May 2021) under a CC BY 4.0 licence for other researchers to use [10].

The rest of the article is structured as follows. Section 2 presents a short overview of pollen grain segmentation methods. Section 3 presents the data acquisition, quality control and annotation protocol. The segmentation pipeline, as well as the performance results of the method are presented in Sections 4 and 5, respectively. Finally, the findings of the study are discussed in Section 6 and the article is concluded in Section 7.

2. Related Works

Damian et al. [11] proposed a 2-stage segmentation pipeline. In the first stage, they utilized Hough transform in order to detect the initial contours based on a circle-like pattern. After the initial contour estimation, three different methods were compared for the fine detection of the pollens' contours. In particular, they utilized a basic edge-contour approach which was based on the gradient image, the snake-contour algorithm and the convex-hull algorithm. However, not all pollen grains have a circle-like shape as the ones examined in this study, originating from the Urticaceae family, and, thus, their approach may perform poorly on other types of pollen grains.

Battiato et al. [12,13] presented the Pollek13K dataset, which consists of a bit more than 13.000 segmented grains of 5 pollen types, which included a separate class for possible debris. In order to segment each one of the 13k grains, they developed a 3-stage processing pipeline, which consists of a pre-processing stage, the segmentation stage and a post-processing stage. During the preprocessing stage, several noise reduction filters are applied (i.e., mean shift filtering, Gaussian blurring), as well as the Otsu's thresholding method to highlight the foreground and the pollen grains' contours. In order to identify each pollen grain, several morphological operations are used. In addition, having the objects of interest filled with black color while the background filled with white color, any detected object that was smaller or larger than a predefined minimum or maximum size was discarded from the final dataset, based on analyzing the connected components in the image. Finally, in order to highlight only the foreground (i.e., the object of interest) in each of the segmented images and discard any of the background information, a post-processing approach based on several noise reduction filters and morphological operations was used. When we applied this processing pipeline on our data, we found that, although it performs well on large or well separated pollen grains, it really struggles to identify overlapping ones.

Olsson et al. [14] developed a pollen grain segmentation pipeline which is based on watershed algorithm. Prior to the application of the watershed algorithm, the image applied a threshold, as well as several morphological operations [15], similarly to the previously mentioned approaches.

Finally, Gallardo et al. [16] developed a pollen grain detection method based on a convolutional neural network (CNN). Their CNN was trained based on a multifocal analysis approach, in which several focus points were used on the camera in order to capture all pollen grains under the optimal focus setting. The camera captured a video across all the focus points, which was used to train the network, after annotating a bounding box around each of the pollen grains. Their approach was trained and tested on 11 different pollen types and outperformed other methods that were based on non-machine learning image processing techniques, achieving recall and precision scores of 99% and intersection over union (IoU) score of 0.9. However, two main drawbacks of this approach is the laborious and time-consuming process of capturing the video, as well as annotating each grain at the various focus points.

In this study, we present a novel pipeline for segmenting pollen grains from fuchsin-stained microscope images of 20 types of plants gathered in Crete, Greece. The novelty of this study is twofold. First, the proposed method is robust and accurate since it is able to correctly detect and segment pollen grains of various shapes and sizes. Secondly, the proposed dataset is a unique and novel collection of pollen grains from plants across Crete, Greece, which we hope that this will accelerate the development of automated machine learning and deep learning systems for pollen classification, which is an essential step for melissopalynology and honey certification.

3. Data

3.1. Image Acquisition

Microscopic slides were prepared from freshly cut flowers collected from various places of Crete during April 2019 to April 2021. Before extracting pollen, plant species were identified by a botanist. Pollen was isolated in the laboratory to create permanent microscope preparations according to [2]. On a 76 × 26 glass slide (Objektträger knittel, Germany), one drop of filtered honey:water solution (2:1) was spread and the anthers of each plant were shaken over it so that the pollen would fall. Subsequently, a solution of 0.05% Pararosaniline chloride (Acros Organics, India) in ethanol was added as a colouring agent. The slides were placed in a heating hearth, at 40°C to evaporate the moisture, followed by covering the sample with cover slips (Objektträger knittel, Germany) and mounting medium (Eukitt Quick, Sigma-Aldrich, Germany). Permanent pollen preparations were allowed to dry before storage. Subsequently, the images of the samples were captured using a Leica CME microscope using an external Canon Power Shot A620 camera. The images were taken at magnification of ×400.

3.2. Image Quality Control

However, some samples, like the one in Figure 1, have too many overlapping pollens, as well as debris, which can be seen as black spots or a pink dyed area (as at the top right corner). Such images were discarded due to their poor quality.

3.3. Image Annotation

After the acquisition and the quality control stages, each image was annotated by drawing the bounding box of each pollen grain. An example of such annotation can be seen in Figure 2. Doing so, it is possible to assess the performance of the segmentation, by comparing the predicted bounding boxes with the ground truth. In particular, if the IoU between the predicted bounding box and the ground truth is above a certain threshold (i.e., 50%), the predicted pollen is considered to be correctly detected.

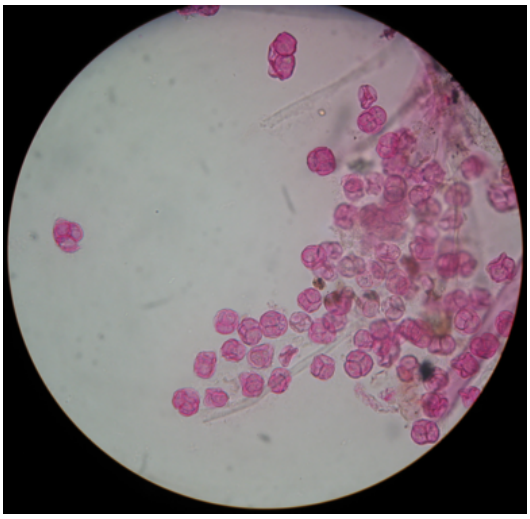

Figure 1. Bad quality image example.

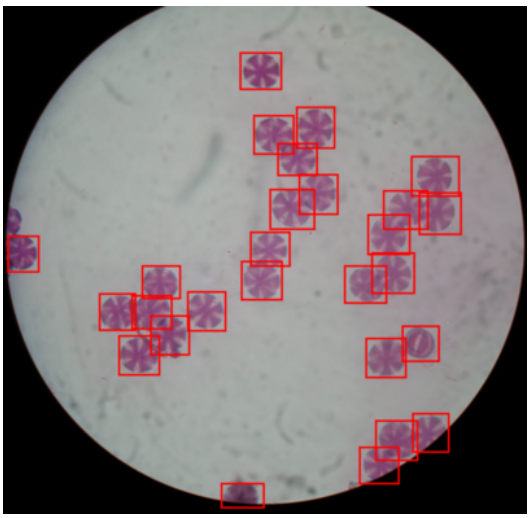

Figure 2. Annotated image example.

4. Segmentation Pipeline

In this section, we present and describe in detail the pollen grain segmentation pipeline. The term "segmentation" in image processing and computer vision refers to the process of identifying, locating, and partitioning segments of the image that are of particular interest (i.e., the pollen grains in this case). In this study, the segmentation pipeline consists of 3 main components, which are also presented in Figure 3:

1. Image pre-processing;
2. Pollen grain segmentation;
3. Pollen grain image post-processing.

The method was implemented in Matlab using the Image Processing Toolbox on a Ryzen 7 3700× CPU with 32 GB 3200 MHz RAM. The processing time for a single image was 1–2 seconds, depending on the number of unique pollen grains in the image. It should be noted that the preprocessing and segmentation stages of the pipeline are based on a semi-automatic approach, in the sense that several hyper-parameters can be tuned by the user during the execution of the methods, such as the morphological operations' parameters.

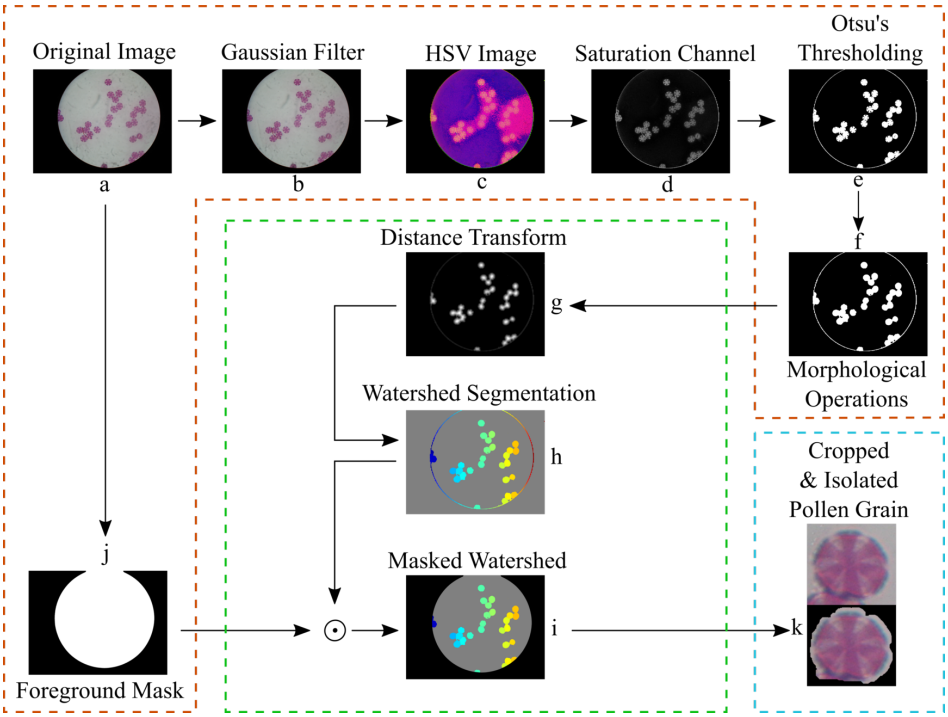

Figure 3. The segmentation pipeline: pre-processing stage (orange), segmentation stage (green), and post-processing stage (blue). Each specific stage corresponds to: a) the original image, b) the gaussian filtered image, c) the corresponding HSV image, d) the saturation channel of the HSV image, e) the image after the threshold was applied, f) the image after the morphological operations were applied, g) the distance transform result, h) the segmentation map as calculated by the watershed algorithm, i) the masked segmentation map, j) the foreground mask and k) examples of a cropped (with background present) and an isolated (with background discarded) pollen grain.

4.1. Pre-Processing Stage

The aim of the preprocessing stage of the pipeline is to decrease any noise that may be present in the raw images and highlight the pollen grains' contours that will be used for segmenting them. Firstly, we apply a Gaussian blurring filter (Equation (1)) in order to eliminate any high-frequency noise and smooth the image.

$$G(x) = \frac{1}{2\pi\sigma^2} \exp - \frac{x^2 + y^2}{2\sigma^2} \tag{1}$$

where σ is the standard deviation of the Gaussian distribution, which was set to $\sigma = 0.5$, and x, y are the pixel's coordinates in the 2D plane. Then we convert the image from the red-green-blue (RGB) color model to the hue-saturation-value (HSV) model, Equations (2)–(5), and extract the saturation channel.

$$\begin{aligned} M &= max(R, G, B) \\ m &= min(R, G, B) \\ C &= M - m \end{aligned} \tag{2}$$

$$Hue = 60° \begin{cases} undefined, & if C = 0 \\ \frac{G-B}{C} mod 6, & if M = R \\ \frac{B-R}{C} + 2, & if M = G \\ \frac{R-G}{C} + 4, & if M = B \end{cases} \tag{3}$$

$$Saturation = \begin{cases} 0, & if V = 0 \\ \frac{C}{V}, & otherwise \end{cases} \tag{4}$$

$$Value = max(R, G, B) = M \tag{5}$$

Because of the staining protocol, the pollen grains have a higher saturation value than the background does. Thus, by extracting the saturation channel from the HSV image, the pollen grains are better illuminated than they are on the RGB image, as seen in Figure 3d. After the extraction of the saturation channel, the Otsu's thresholding filter is applied [17]. Finally, an opening or closing morphological operations or a combination of them is used in order to (**a**) reduce any salt and pepper noise (i.e., white and black spots) that may be present after the thresholding or (**b**) to fill any gaps within the pollen grains (Figure 3e). In addition, we produce a foreground mask, as seen in Figure 3j, by converting the RGB image to its grayscale equivalent (Equations (6)) and thresholding it at the value of 20.

$$Grayscale = 0.2989 * R + 0.5870 * G + 0.1140 * B \tag{6}$$

Similarly to the previous thresholding operation, in order to reduce any salt and pepper noise and fill any gaps, we apply several morphological operations (i.e., opening and closing, respectively). Finally, we shrink the generated mask, in order to make the binary circle mask a bit smaller, by applying an eroding morphological operation. This mask will be used to discard the outer part of the visible section of the image, which is shadowed and does not hold any meaningful information for the segmentation stage, as seen in Figure 3i.

4.2. Segmentation Stage

The segmentation is based on the watershed algorithm, which is able to highlight even overlapping pollen grains fairly accurately. As seen in Figure 3, the input to the segmentation stage is the thresholded image from the previous stage and the foreground mask. The first step is to calculate the distance transform of the complement of the thresholded image. The value of each pixel of the distance transform is calculated as the distance between that pixel and the nearest non-zero pixel of the complement of the thresholded image. Then the watershed algorithm is applied on the complement image of the distance transform. The resulting image from the watershed algorithm is multiplied pixel-wise by the foreground mask, in order to reduce any artifacts around the edge, that may be identified as pollen grains by the algorithm, as seen in Figure 3h,i. Having the result of the watershed algorithm, we extract the contours of each identified pollen grain and analyze their morphology. Doing so, we calculate the area of each pollen grain in pixels, its centroid, as well as the bounding box surrounding its contour.

4.3. Post-Processing Stage

Having extracted the contour and the binary mask of each pollen grain, as well as having calculated their morphological characteristics, we can analyze them in order to discard any duplicate or false-positive pollen grains. Firstly, we identify possible duplicates by comparing the coordinates and possible overlaps between the computed bounding boxes for each of the pollen grains. If two bounding boxes with similar centroids' coordinates overlap by at least 80%, then one of them is discarded as a duplicate of the other. Then we discard any detected pollen grain, whose contour area is bigger or smaller than two pre-specified values. The pollen grain size varies across the different types of pollens, as can be seen in Figure 4. As an optional step, each segmented pollen grain is multiplied pixel-wise by its binary mask, in order to discard the background and keep only the foreground of each individual pollen grain, as seen in the last stage of the pipeline in Figure 3k. In order to distinguish between the two, the segmented pollen grains whose background has been discarded will be referred as "isolated pollen grains" from now on, while those with the background present will be referred as "cropped pollen grains".

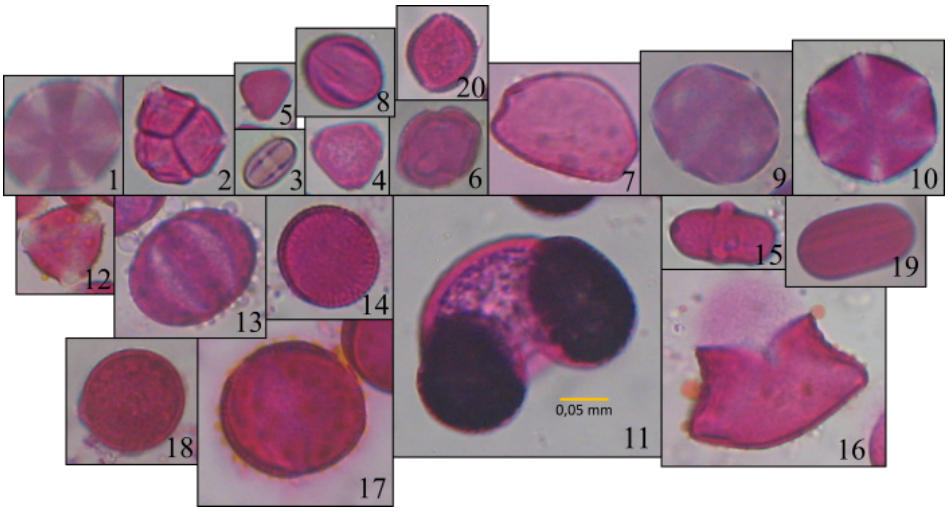

Figure 4. A mosaic of all segmented pollen grains, numbered as in Table 1.

5. Results

The performance of the segmentation pipeline is reported in Table 1. In particular, there are two metrics that are presented, i.e., the number of the detected pollen grains and the method's accuracy for detecting pollen grains for each one of the pollen types. The performance results in Table 1 shows that the proposed method can detect each individual pollen grain with a high accuracy across all types of pollen. In addition, the proposed dataset consists of more than 4000 unique pollen grains from 20 types of plants, making it the second largest publicly available pollen dataset and the largest one regarding pollen that has been collected directly from plants, as seen in Table 2.

Table 1. Method performance results.

ID	Plant Name	Detected	Accuracy	ID	Plant Name	Detected	Accuracy
1	*Thymbra*	146	98.7%	11	*Pinus*	29	100%
2	*Erica*	181	97.3%	12	*Calicotome*	298	94.0%
3	*Castanea*	218	81.0%	13	*Salvia*	178	96.7%
4	*Eucalyptus*	170	97.1%	14	*Sinapis*	197	97.5%
5	*Myrtus*	786	79.4%	15	*Ferula*	83	90.2%
6	*Ceratonia*	100	96.1%	16	*Asphodelus*	34	100%
7	*Urginea*	109	99.1%	17	*Oxalis*	139	96.5%
8	*Vitis*	269	95.4%	18	*Pistacia*	34	100%
9	*Origanum*	171	99.4%	19	*Ebenus*	22	100%
10	*Satureja*	71	100%	20	*Olea*	790	92.9%

Table 2. Comparison between the available datasets.

Dataset	# Pollen Types	# Grains	Image Type	Resolution	Magnification	Staining	Origin	Region
Proposed	20	4034	Color	Varying	40x	Fuchsin	Plants	Crete, Greece
Pollen13K [13]	3 + Debris	∼13.000	Color	84x84	N/A	Fuchsin	Airborne Samples	N/A
POLEN23E [18]	23	790	Color	Varying	40x	N/A	Honey	Brazilian Savanna
POLLEN73S [19]	73	2523	Color	Varying	40x	Fuchsin	Plants	Brazilian Savanna

Regarding the *Myrtus* pollen grains, which were detected with a low accuracy of 79.4%, there was a dense concentration of pollen grains in the images, with many overlaps and occlusions, as seen in Figure 5. Such overlaps and occlusions make it difficult for the method to properly distinguish each unique pollen grain. A similar problem is observed on the *Castanea* pollen grains, as seen in Figure 6, on which the detection accuracy was 81%. These particular pollen grains have a very small size as can be seen in Figure 4-3 and Figure 6, compared to the rest pollen types. Thus, their small size combined with possible overlaps, make their detection trickier. However, there are more than 1000 and 200 pollen grains detected for each pollen type, respectively, which can be enough for a classification analysis when their unique shape and characteristics, as well as the number of the detected pollen grains of the rest species are also considered.

Although there is an imbalance for some pollen types, such as *Pinus* (Figure 4-11) and *Asphodelus* (Figure 4-16) their shape and characteristics are unique when compared to the rest of the pollen types. Thus, we do not expect a great performance loss in a machine learning classification task regarding these pollen classes. Similarly, we do not expect much performance issues when the *Ebenus* (Figure 4-19) pollen is considered, due to its similar size and shape to the *Ferula* (Figure 4-15) pollen. The former is rather smooth both on its outline and within it, in contrast to the latter, which has a rather harsher outline and texture. On the other hand, the same does not apply for the *Pistacia* pollen (Figure 4-18), which has a very similar shape and texture with other pollen types, such as *Sinapis* (Figure 4-14). As a result, we expect that these pollen types will be harder to distinguish from one another. In order to deal with such imbalancing, and increase the data, image augmentation techniques can be used.

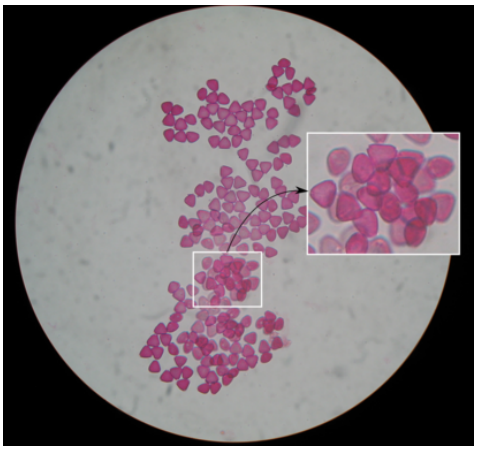

Figure 5. Image example showing some missed pollen grains due to multiple occlusions for the *Myrtus* species.

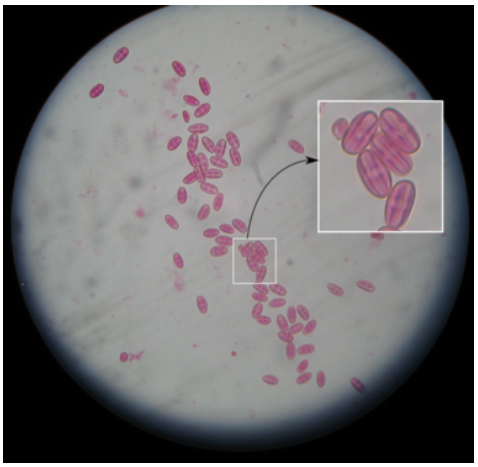

Figure 6. Image example showing some missed pollen grains for the *Castanea* species.

6. Discussion

Although for most cases the segmentation masks enclose the whole pollen grain, there are some cases where part of the pollen grain has been removed. In order for the reader to fully understand this issue, Figure 7 presents an example of a correctly segmented pollen grain (Figure 7a) and a poorly segmented one (Figure 7b). Such poorly segmented pollen grains encountered in images with dense concentration of pollen grains, i.e., *Thymbra*, *Eucalyptus*, *Myrtus*, etc. In addition, there are very few cases in densely concentrated microscopic images, where an isolated pollen grain image contains part of a separate pollen grain (Figure 7c). Table 3 presents the proportion of poorly segmented pollen grains for each class, respectively. It can be observed that *Thymbra*, which is the most characteristic pollen type of the honey product of interest, has a proportion of 6.5% of poorly segmented pollen grains. However, we estimate that this issue will not have a serious impact on the performance of any machine learning based classification method, since they are only a small percentage of the dataset size when considering the size of each class individually. In addition, modern image augmentation techniques can be used to generate more samples and increase the size of the dataset.

Table 3. Proportion of poorly segmented pollen grains.

ID	Plant Name	Proportion	ID	Plant Name	Proportion
1	*Thymbra*	6.5%	11	*Pinus*	0%
2	*Erica*	1.7%	12	*Calicotome*	2.3%
3	*Castanea*	1.8%	13	*Salvia*	3.4%
4	*Eucalyptus*	1.8%	14	*Sinapis*	1%
5	*Myrtus*	3.8%	15	*Ferula*	2.4%
6	*Ceratonia*	3%	16	*Asphodelus*	2.9%
7	*Urginea*	1.8%	17	*Oxalis*	0.7%
8	*Vitis*	3%	18	*Pistacia*	0%
9	*Origanum*	2.3%	19	*Ebenus*	0%
10	*Satureja*	0%	20	*Olea*	1.3%

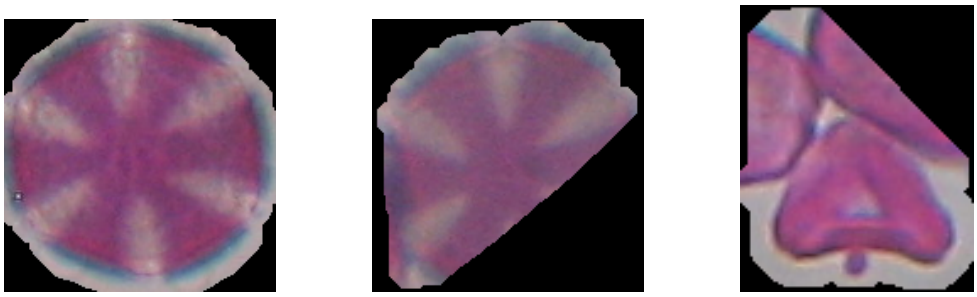

(a) **(b)** **(c)**

Figure 7. (**a**) proper segmentation example, (**b**) poor segmentation example and (**c**) an example of an isolated pollen grain image which wrongfully includes part of other pollen grains.

In a future study, a more advanced image capturing device will be used (i.e., Kern microscope with built-in camera ODC-82/ODC-83, Kern, Germany) which will produce images of higher quality with less illumination artifacts than the ones used in this study. In addition, a deep learning based detection method will be explored, in order to increase both the detection accuracy, as well as the segmentation quality of the method.

7. Conclusions

This article presents the Cretan Pollen Dataset v1 (CPD_v1), which comprises microscope images of stained pollen grains of 20 plant types. A segmentation method based on the watershed algorithm was developed to segment each unique pollen grain, with an overall accuracy of 92%. The complete dataset with the raw data, the ground truth annotations, and the segmented pollen grains are also publicly available at 10.5281/zenodo.4756360 (accessed on 13 May 2021), as presented in Table 4, for other researchers to use [10].

Table 4. List of data available in the dataset (10.5281/zenodo.4756360 accessed on 13 May 2021).

Data	Description	#	Data Type	File Format
Color Microscope Images	Raw data	157	Image	png
Pollen Annotations	Bounding boxes of pollen grains	20	Tabular	CSV
Cropped Pollen Grains	Segmented pollen grains with the background	4034	Image	png
Isolated Pollen Grains	Segmented pollen grains without the background	4034	Image	png

Author Contributions: Conceptualization, N.T., G.M., K.M., and E.A.; methodology, N.T., G.M., and K.M.; software, N.T. and S.K.; validation, N.T. and E.S.; formal analysis, N.T. and E.S.; investigation, N.T. and E.S.; resources, E.S. and E.A.; data curation, N.T., E.S., and E.A.; writing—original draft preparation, N.T., E.S., and G.M.; writing—review and editing, N.T., N.V., K.M., and E.A.; visualization, N.T.; supervision, N.V., K.M., and E.A.; project administration, E.A.; funding acquisition, N.V. and E.A. All authors have read and agreed to the published version of the manuscript.

Funding: This research was funded by the Emblematic Action "The Honeybee Roads" of the Greek Public Investments Program (P.I.P.) of General Secretariat for Research and Technology (GSRT) (project code: 2018Σ*E*01300000).

Institutional Review Board Statement: Not applicable.

Informed Consent Statement: Not applicable.

Data Availability Statement: The data presented in this study are openly available in Zenodo at 10.5281/zenodo.4756360 (accessed on 13 May 2021).

Conflicts of Interest: The authors declare no conflicts of interest.

References

1. Soares, S.; Amaral, J.S.; Oliveira, M.B.P.; Mafra, I. A comprehensive review on the main honey authentication issues: Production and origin. *Compr. Rev. Food Sci. Food Saf.* **2017**, *16*, 1072–1100. [CrossRef] [PubMed]
2. Von Der Ohe, W.; Oddo, L.P.; Piana, M.L.; Morlot, M.; Martin, P. Harmonized methods of melissopalynology. *Apidologie* **2004**, *35*, S18–S25. [CrossRef]
3. Louveaux, J.; Maurizio, A.; Vorwohl, G. Methods of melissopalynology. *Bee world* **1978**, *59*, 139–157. [CrossRef]
4. Dunker, S.; Motivans, E.; Rakosy, D.; Boho, D.; Maeder, P.; Hornick, T.; Knight, T.M. Pollen analysis using multispectral imaging flow cytometry and deep learning. *New Phytol.* **2021**, *229*, 593–606. [CrossRef] [PubMed]
5. Sevillano, V.; Aznarte, J.L. Improving classification of pollen grain images of the POLEN23E dataset through three different applications of deep learning convolutional neural networks. *PLoS ONE* **2018**, *13*, e0201807. [CrossRef] [PubMed]
6. Sevillano, V.; Holt, K.; Aznarte, J.L. Precise automatic classification of 46 different pollen types with convolutional neural networks. *PLoS ONE* **2020**, *15*, e0229751. [CrossRef] [PubMed]
7. Geographical Indications: An Introduction. Available online: https://www.wipo.int/publications/en/details.jsp?id=272 (accessed on 13 May 2021).
8. Török, Á.; Jantyik, L.; Maró, Z.M.; Moir, H.V. Understanding the Real-World Impact of Geographical Indications: A Critical Review of the Empirical Economic Literature. *Sustainability* **2020**, *12*, 9434. [CrossRef]
9. Pefkothymaromelo Kritis, P.D.O. Specifications. Available online: http://www.minagric.gr/images/stories/docs/agrotis/POP-PGE/prod_pefkothimaromelo_kriti.pdf (accessed on 13 May 2021).
10. Tsiknakis, N.; Savvidaki, E.; Kafetzopoulos, S.; Manikis, G.; Vidakis, N.; Marias, K.; Alissandrakis, E. Cretan Pollen Dataset **2021**. [CrossRef]
11. Rodriguez-Damian, M.; Cernadas, E.; Formella, A.; Fernández-Delgado, M.; De Sa-Otero, P. Automatic detection and classification of grains of pollen based on shape and texture. *IEEE Trans. Syst. Man Cybern. Part C (Appl. Rev.)* **2006**, *36*, 531–542. [CrossRef]
12. Battiato, S.; Ortis, A.; Trenta, F.; Ascari, L.; Politi, M.; Siniscalco, C. Detection and classification of pollen grain microscope images. In Proceedings of the IEEE/CVF Conference on Computer Vision and Pattern Recognition Workshops, Seattle, WA, USA, 14–19 June 2020; pp. 980–981.
13. Battiato, S.; Ortis, A.; Trenta, F.; Ascari, L.; Politi, M.; Siniscalco, C. Pollen13K: A Large Scale Microscope Pollen Grain Image Dataset. In Proceedings of the 2020 IEEE International Conference on Image Processing (ICIP), Abu Dhabi, United Arab Emirates, 25–28 October 2020; pp. 2456–2460.
14. Olsson, O.; Karlsson, M.; Persson, A.S.; Smith, H.G.; Varadarajan, V.; Yourstone, J.; Stjernman, M. Efficient, automated and robust pollen analysis using deep learning. *Methods Ecol. Evol.* **2021**, *12*, 850–862. [CrossRef]
15. Najman, L.; Talbot, H. *Mathematical Morphology: From Theory to Applications*; John Wiley & Sons: Hoboken, NJ, USA, 2013.
16. Gallardo-Caballero, R.; García-Orellana, C.J.; García-Manso, A.; González-Velasco, H.M.; Tormo-Molina, R.; Macías-Macías, M. Precise pollen grain detection in bright field microscopy using deep learning techniques. *Sensors* **2019**, *19*, 3583. [CrossRef] [PubMed]
17. Otsu, N. A threshold selection method from gray-level histograms. *IEEE Trans. Syst. Man Cybern.* **1979**, *9*, 62–66. [CrossRef]
18. Gonçalves, A.B.; Souza, J.S.; Silva, G.G.d.; Cereda, M.P.; Pott, A.; Naka, M.H.; Pistori, H. Feature extraction and machine learning for the classification of Brazilian Savannah pollen grains. *PLoS ONE* **2016**, *11*, e0157044. [CrossRef] [PubMed]
19. Astolfi, G.; Gonçalves, A.B.; Menezes, G.V.; Borges, F.S.B.; Astolfi, A.C.M.N.; Matsubara, E.T.; Alvarez, M.; Pistori, H. POLLEN73S: An image dataset for pollen grains classification. *Ecol. Inform.* **2020**, *60*, 101165. [CrossRef]